DOI:10.1093/jnci/djt022
Advance Access publication February 15, 2013

ARTICLE

A Cancer Stem Cell Model for Studying Brain Metastases From Primary Lung Cancer

Sara M. Nolte, Chitra Venugopal, Nicole McFarlane, Olena Morozova, Robin M. Hallett, Erin O'Farrell, Branavan Manoranjan, Naresh K. Murty, Paula Klurfan, Edward Kachur, John P. Provias, Forough Farrokhyar, John A. Hassell, Marco Marra, Sheila K. Singh

Manuscript received May 30, 2012; revised October 1, 2012; accepted January 4, 2013.

Correspondence to: Sheila K. Singh, MD, PhD, FRCS(C), Department of Surgery, McMaster Children's Hospital, and McMaster Stem Cell and Cancer Research Institute, McMaster University, MDCL 5072, 1280 Main St W, Hamilton, ON L8S 4K1, Canada (e-mail: ssingh@mcmaster.ca).

Background Brain metastases are most common in adults with lung cancer, predicting uniformly poor patient outcome, with a median survival of only months. Despite their frequency and severity, very little is known about tumorigenesis in brain metastases.

Methods We applied previously developed primary solid tumor-initiating cell models to the study of brain metastases from the lung to evaluate the presence of a cancer stem cell population. Patient-derived brain metastases (n = 20) and the NCI-H1915 cell line were cultured as stem-enriching tumorspheres. We used in vitro limiting-dilution and sphere-forming assays, as well as intracranial human–mouse xenograft models. To determine genes overexpressed in brain metastasis tumorspheres, we performed comparative transcriptome analysis. All statistical analyses were two-sided.

Results Patient-derived brain metastasis tumorspheres had a mean sphere-forming capacity of 33 spheres/2000 cells (SD = 33.40) and median stem-cell frequency of 1/60 (range = 0–1/141), comparable to that of primary brain tumorspheres ($P = .53$ and $P = .20$, respectively). Brain metastases also expressed CD15 and CD133, markers suggestive of a stemlike population. Through intracranial xenotransplantation, brain metastasis tumorspheres were found to recapitulate the original patient tumor heterogeneity. We also identified several genes overexpressed in brain metastasis tumorspheres as statistically significant predictors of poor survival in primary lung cancer.

Conclusions For the first time, we demonstrate the presence of a stemlike population in brain metastases from the lung. We also show that NCI-H1915 tumorspheres could be useful in studying self-renewal and tumor initiation in brain metastases. Our candidate genes may be essential to metastatic stem cell populations, where pathway interference may be able to transform a uniformly fatal disease into a more localized and treatable one.

J Natl Cancer Inst;2013;105:551–562

Brain metastases are common in adults suffering from a variety of primary cancers, including those of the lung, breast, and colon (1). Up to 50% of lung cancer patients develop brain metastases, the majority within a few years of diagnosis (2–5). Due to their subcortical location, lung-derived brain metastases are less easily surgically excised than the dural-based metastases, typical of breast cancer (6). Their invasive nature and ability to escape current treatments predicts uniformly poor patient outcome, with a median survival time of only months (7, 8). Despite the frequency and severity, very little research exists on brain metastases from lung cancer, nor is there an appropriate experimental model with which to study them.

The application of a cancer stem cell (CSC) model to primary tumorigenesis has shown that a rare subpopulation of tumor cells is responsible for the initiation and maintenance of the tumor (9–14). These tumor-initiating cells (TICs) have been identified by several markers (CD133 [11, 12, 15, 16], CD15 [10, 13], $CD44^{hi}/CD24^{lo}$ [17], and aldehyde dehydrogenase [ALDH] activity [9, 14, 18–22]), where brain tumor-initiating cells (BTICs) are capable of self-renewal and producing all cells found within the heterogeneous tumor. Whereas CD133 (15) and ALDH activity (22) have been used to identify TIC populations in small cell and non–small cell lung cancers, it has also been suggested that the different lung cancer subtypes (eg, adenocarcinoma, squamous cell carcinoma) may arise from the normal progenitors or stem cells of the local area (eg, bronchioalveolar stem cells [23, 24], basal progenitors [25], respectively). However, the heterogeneity of lung cancer subtypes has likely contributed to the lack of a common in vitro or in vivo model, precluding the study of brain metastases from the lung.

The idea of a subpopulation of cells initiating tumor growth is quite similar to the metastatic process (26). Although many cells may be shed from the primary tumor, only a small number of cells are able to survive in the circulation and seed a secondary site (27, 28). An even

smaller number are able to propagate in a new niche into a clinically apparent tumor (27, 28). In fact, many studies have reported increased adhesion and invasiveness in CSCs of various primary tumor models, implicating the involvement of CSCs in the development of metastases (29–33). These observations, the metastatic process, and existence of CSCs in lung cancer led us to hypothesize that brain metastases from the lung may also arise from a TIC population.

A stem cell population can be identified through assessment of self-renewal in vitro, and through serial passage and tumor recapitulation in vivo (34). In the current study, patient tumor samples and cell lines were cultured as tumorspheres in neural stem cell (NSC) conditions to enrich for stemlike populations. Using sphere-forming assays to assess self-renewal, we show that brain metastases from the lung possess sphere-forming capacities similar to those of primary brain tumors. Intracranial injection of minimally cultured, patient-derived, and NCI-H1915 tumorspheres into nonobese diabetic severe combined immunodeficient (NOD-SCID) mice demonstrated similar multifocal tumor formation, and recapitulated tumor cytoarchitecture and heterogeneity, indicating that NCI-H1915 cells can be used as a surrogate for patient samples in vivo. We also used serial intracranial injection of NCI-H1915 tumorspheres into NOD-SCID mice to show that the putative TIC population can be serially passaged.

We performed RNA-sequencing (RNA-Seq) and subsequent comparative analysis of brain metastasis tumorspheres, primary lung and brain tumors, to identify genes overexpressed in stem cell–enriched brain metastases. These candidate genes predicted decreased survival in primary lung cancer patients, and are known to be involved in cell adhesion, cytoskeleton rearrangements, proliferation/tumorigenesis, and formation/disruption of cell–cell junctions. Further characterization of these genes in pathways essential for the metastasis of lung cancer to the brain may prove to be useful and effective as therapeutic targets.

Methods

Patient Sample Processing and Cell Culture

Consecutive brain tumor samples (1–2 cm^3) were collected from consenting patients undergoing surgical tumor resection (Hamilton Health Sciences Research Ethics Board, #07-366). Specimens pathologically diagnosed as lung-derived brain metastases from patients with a history of lung cancer were used in the study (n = 20), alongside primary brain tumor controls (n = 3). Nonviable samples were excluded from the study, as defined by failure to propagate as tumorspheres, ≥80% cell death, and pathological diagnosis of high necrotic tissue content (approximately 20% of all samples collected). Upon collection, samples were mechanically dissociated and subjected to enzymatic digestion with 200 µL Liberase Blendzyme (0.2 Wunisch units/mL, Roche) for 15 minutes at 37°C on an incubator rocker (VWR). Undigested tissue was removed, and red blood cells were lysed (RBC Lysis Buffer, Stem Cell Technologies). Cells were washed with phosphate-buffered saline (Hyclone), subsequently resuspended in complete NSC (cNSC) media, and plated in an ultra-low attachment plate (Corning). Complete NSC media is comprised of NSC basal media (1% N2 supplement [Gibco], 0.2% 60 µg/mL *N*-acetylcystine, 2% neural survival factor-1 [Lonza], 1% HEPES, and 6 mg/mL glucose in 1:1 Dulbecco's Modified Eagle Medium and F12 media [Gibco]), supplemented with 1× antibiotic–antimycotic (Wisent), 20 ng/mL human epidermal growth factor (Sigma), 20 ng/mL basic fibroblast growth factor (Invitrogen), and 10 ng/mL leukemia inhibitory factor (Chemicon). We also used two cell lines cultured in cNSC media: NCI-H1915 (American Type Culture Collection) cells were isolated from a brain metastasis of a 61-year-old woman with a large cell, poorly differentiated lung carcinoma; BT241 is a lab-derived glioblastoma (GBM) cell line from a 68-year-old woman. Cultures were maintained at 37°C, 5% CO_2, and media was changed every other day, or as needed.

Sphere Formation Assay and Limiting Dilution Analysis

Tumorspheres were dissociated using 5–10 µL Liberase Blendzyme in 1 mL of phosphate-buffered saline for 5 minutes at 37°C. Cells were plated at limiting dilution (200 to 2 cells per well) in 100 µL of cNSC media in quadruplicate in a 96-well plate. After seven days, the number of spheres per well was counted for each dilution, and was used to estimate the mean number of spheres per 2000 cells. For patient samples, this assay estimated secondary sphere formation, whereas cell lines were passage three or higher. The fraction of negative wells vs cell dilution was graphed and fitted with a linear regression to estimate stem cell frequency, as in Tropepe et al (35). Following the assumption that a single stem cell gives rise to one sphere (36), the proportion of negative wells can be defined by the zero point (F_0) of the Poisson distribution: $F_0 = e^{-x}$, where x is the mean number of cells per well. The dilution at which it is expected to have one stem cell (one sphere) per well can be identified by the point at which the line-of-best-fit crosses 0.37 (when $x = 1$, $F_0 = e^{-1} = 0.37$) (35).

Flow Cytometry and Cell Sorting

The Aldefluor assay (Stem Cell Technologies) was used as a nonimmunological method to analyze the ALDH activity of samples, where high enzyme activity is an indication of stem cell populations. Cells were also stained and assessed for surface expression of CD15 and CD133 by flow cytometry (Supplementary Materials, available online). Cells were sorted (purify settings) into tubes of NSC basal media and allowed to equilibrate at 37°C for 1–2 hours after sorting, prior to their use in experiments. Aliquots of sorted populations were taken for purity assessment immediately after sorting. For clonal analysis of single cells, $CD15^+$ or $CD15^-$ cells were sorted one cell per well of a 96-well plate into 100 µL of 25% NCI-H1915 conditioned cNSC media. Cultures were left undisturbed for 7 days after sorting, and received an additional 50 µL of cNSC media after 7 days.

Statistical Analyses

Gene Signature Survival Analyses. Genes found to be overexpressed in brain metastases (Supplementary Materials, available online) were ranked according to their ability to predict patient survival in a dataset of 226 primary lung tumor samples (GSE31210) (37) using a median cut-point to calculate hazard ratios and perform log-rank tests. In brief, raw Affymetrix.CEL files (Affymetrix Human Genome U133A Array) and associated clinical data were downloaded from the Gene Expression Omnibus (http://www.ncbi.nlm.nih.gov/geo/; GSE31210), and normalized using robust multi-array analysis (38). Probe expression levels were transformed into

standard normal deviates; patient gene scores were calculated as the mean of the standardized scores from the probe sets undergoing analysis (39–40). Genes producing a log-rank test of *P* less than or equal to .05 (two-sided) were considered to be statistically significantly associated with length of survival. We used Cox proportional hazards regression to complete forward selected stepwise regression to identify an optimal model for predicting patient outcome. Kaplan–Meier survival analysis was performed, where the patient cohort was divided into tertiles to discriminate patients into high, medium, or low expression groups.

Other Experiments. Statistical analyses were performed using GraphPad Prism 5. Two-sided *t* tests were used, and data are presented as mean (SD), unless otherwise stated. Survival curve analysis for in vivo experiments was performed using the log-rank (Mantel-Cox) test. Statistical significance was set at *P* less than .05 (two-sided).

Results

Patient-Derived Brain Metastases and NCI-H1915 Cells Form Stem-Enriched Tumorspheres and Exhibit Self-Renewal Capacity

It has previously been shown that several cancers, such as breast (17–19), colon (16, 18, 20), lung (15–22), and brain (10–14) tumors possess TIC subpopulations. The presence of these TIC populations has a strong correlation with the development of metastases (29–33). On the basis of these observations, and the fact that brain metastases derive from a limited number of primary tumor cells (27, 28), we wondered whether brain metastases also possessed a self-renewing stemlike population.

Patient samples of primary brain tumors and lung-derived brain metastases were cultured as tumorspheres in cNSC media (Supplementary Table 1, available online). We observed similar secondary sphere-forming capacities between primary brain tumors (19 spheres/2000 cells [SD = 12.55]) and brain metastases (33 spheres/2000 cells [SD = 33.40]; *P* = .53; Figure 1A), where secondary sphere formation is a hallmark of the stem cell property of self-renewal (34). As the brain metastases derived from lung adenocarcinomas, individual cells are much larger and glandular in appearance, resulting in slightly less homogenously spherical and compact tumorspheres, compared to those of primary brain tumors (Figure 1A, lower panels). As a sphere is thought to represent all progeny from a single stem cell, sphere formation reflects the frequency of a stem cell population (35); thus, the presence of tumorspheres is indicative of a culture enriched for stem cells. Stem cell frequency was estimated through limiting-dilution analysis. Median frequencies for patient samples were 1/117 cells (range 1/90–1/160 cells) for primary brain tumors, and 1/60 cells (range 0–1/141 cells) for brain metastases, and were not statistically significantly different (*P* = .20; Figure 1C).

Due to limitations surrounding the use of patient samples (eg, low cell number, low viability, unpredictable acquisition), we supplemented our work with representative cell lines. The NCI-H1915 cell line is derived from a brain metastasis originating from a lung tumor, whereas BT241 is a lab-derived GBM cell line. NCI-H1915 cells, originally grown adherently in RPMI (+10% fetal bovine serum) conditions, were characterized in both RPMI and in cNSC conditions (Supplementary Figure 1, available online). Like their patient-derived counterparts, when in cNSC conditions, both cell lines formed spheres—BT241, 57 spheres/2000 cells (SD = 42.30); NCI-H1915, 217 spheres/2000 cells (SD = 143.50)—and were not statistically significantly different (*P* = .14; Figure 1B); however, their sphere-forming capacity appears to be much higher than that of minimally cultured patient samples. The increased ability to form secondary or higher spheres is likely due to prolonged culture, which can increase stem cell frequency (41, 42), as evidenced by frequencies of 1/78 cells and 1/38 cells for BT241 and NCI-H1915 cultures, respectively (Figure 1D). Despite this increase in sphere-forming capacity, NCI-H1915 and patient-derived brain metastasis tumorspheres were of similar morphology and size (99.07 μm [SD = 16.80] and 163.2 μm [SD = 54.42], respectively; Figure 1E). Together, these data suggest that despite a potential enhanced stem cell compartment in the cell line, NCI-H1915 cells may be appropriate for studying self-renewal in brain metastases, as validated by patient samples.

Known TIC Markers Are Variably Expressed by Patient-Derived and NCI-H1915 Tumorspheres

Primary brain tumor CSC (in vitro) and BTIC (in vivo) populations were previously identified using CD133, CD15, and Aldefluor, where positive populations possess increased self-renewal, hierarchical differentiation, and tumor-initiating capacities (10–14). Both CD133 (15, 16, 18) and Aldefluor (20, 21, 29, 43, 44) have been used to identify TICs in various epithelial cancers, including lung cancer, suggesting that these may be universal markers of stemlike populations in solid tumors. We wondered if these TIC markers were expressed by brain metastases, correlating with the presence of a stemlike population.

We analysed patient-derived tumorspheres for their expression of known brain and lung TIC markers using flow cytometry. All markers selected for subpopulations within the samples, but to varying degrees. $CD133^+$ and $Aldefluor^+$ cells were relatively small populations (9.7% [SD = 11.8] and 10.8% [SD = 15.8], respectively); conversely, CD15 selected for a larger population of cells (39.2% [SD = 33.3]), but with much more variability (Figure 2, A and C).

When looking at the same markers in NCI-H1915 tumorspheres, we found that very few cells were positive for CD133 (0.05% [SD = 0.08]); whereas Aldefluor (36.6% [SD = 20.2]) and CD15 (14.8% [SD = 8.1]) demonstrated much more positivity (Figure 2, B and D). Only CD15 selected for a distinct population (Figure 2D, left panel), in contrast to the absence of $CD133^+$ cells, or whole population shift seen when using Aldefluor (Figure 2D, right panel). CD15 expression was comparable in both NCI-H1915 and patient-derived tumorspheres (Figure 2, A and B); any discrepancies can be attributed to the variability among individual patient tumors. Interestingly, unlike CD133 (15, 16, 18) and Aldefluor (20, 21, 29, 43, 44), CD15 has yet to be shown to select for epithelial TICs, and may be suggestive of a population within the primary tumor primed for growth in the neural microenvironment, as CD15 has previously identified NSC (45) and BTIC (10, 13, 14) populations. Sphere-formation assessment of flow-sorted $CD15^+$ and $CD15^-$ populations from NCI-H1915 tumorspheres indicated no functional difference between the two populations (Supplementary Figure 2, A–E, available online). Flow sorting of patient samples precluded any subsequent experiments.

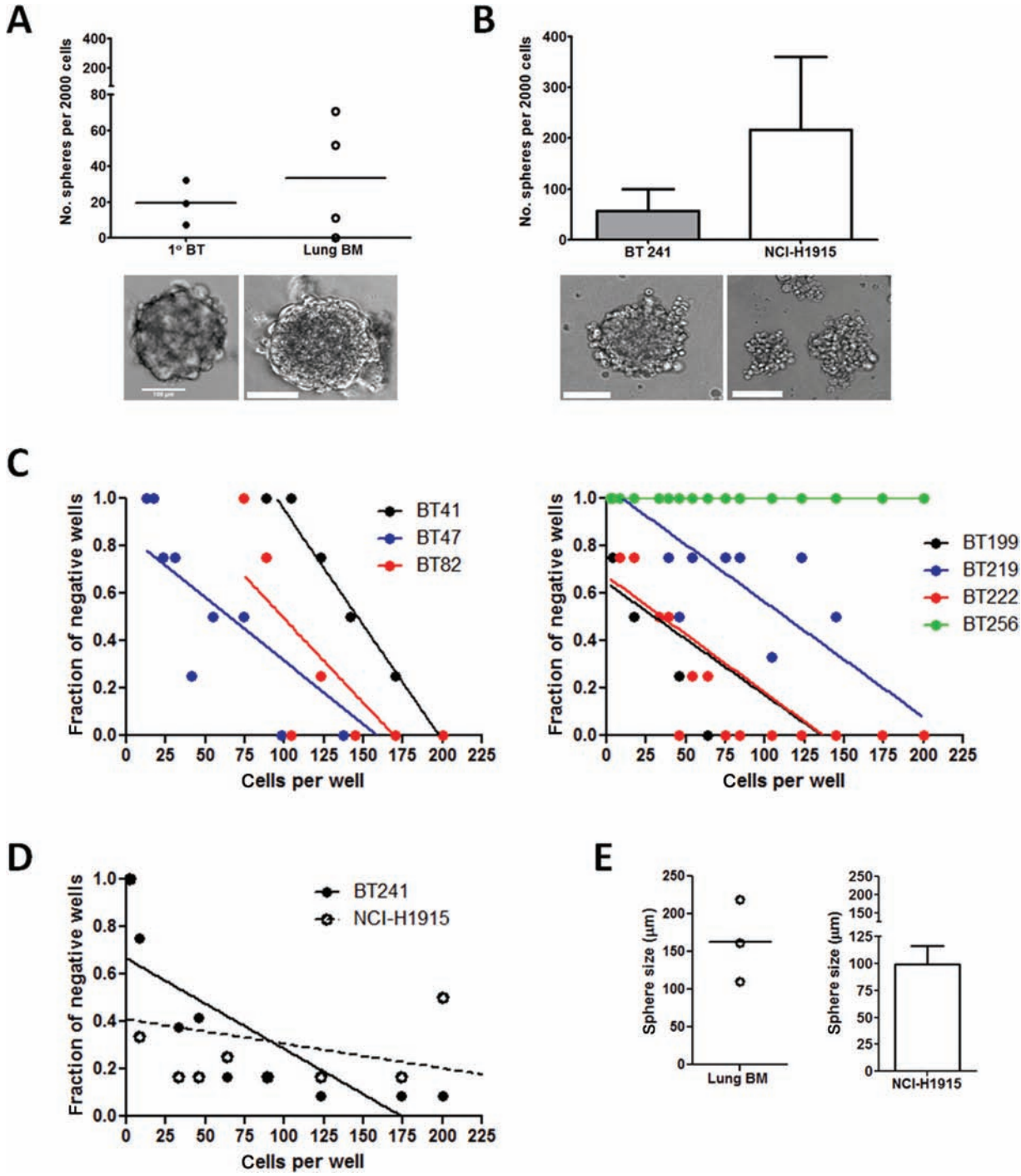

Figure 1. Patient-derived samples and cell lines of primary brain tumors (BTs) and brain metastases (BMs) have similar sphere-forming capacities. Tumorsphere-derived cells were plated at limiting dilution to estimate secondary sphere formation capacity per 2000 cells, averaged over dilutions of 1–200 cells. Corresponding bright-field images of representative spheres are shown below each graph; scale bar is 100 µm. **A)** Sphere formation of patient-derived primary brain tumors (glioblastoma [GBM]; n = 3: BT41, BT47, BT82) and patient-derived brain metastasis samples (from lung; n = 4: BT199, BT219, BT222, BT256), was not statistically significantly different (P = .53). Each dot is representative of one patient sample; bar represents mean of biological replicates. **B)** Sphere formation of cell lines BT241 (GBM cell line) and NCI-H1915 (lung-to-brain metastasis cell line) was not statistically significantly different (P = .14). Results of three independent experiments are shown. **C)** and **D)** Limiting dilution analysis with the zero point of the Poisson distribution $F_0 = e^{-x}$ was used to determine the dilution at which a single stem cell (x = 1, F_0 = 0.37) would give rise to a single tumorsphere, thus estimating stem cell frequency. **C)** Analysis of patient-derived primary brain tumors (**left panel**) and brain metastases (**right panel**). **D)** Analysis of cell lines. A single data point represents the mean of three independent experiments. **E)** Sphere size was measured 7 days after sample collection (patient samples) or passage (NCI-H1915 cell line) for six spheres per sample (**left panel**) or experiment (**right panel**). **Left panel**: each dot represents the mean sphere size for a single patient sample; bar represents mean of biological replicates (n = 3: BT390, BT391, BT397). **Right panel**: results of three independent experiments are shown (n = 3).

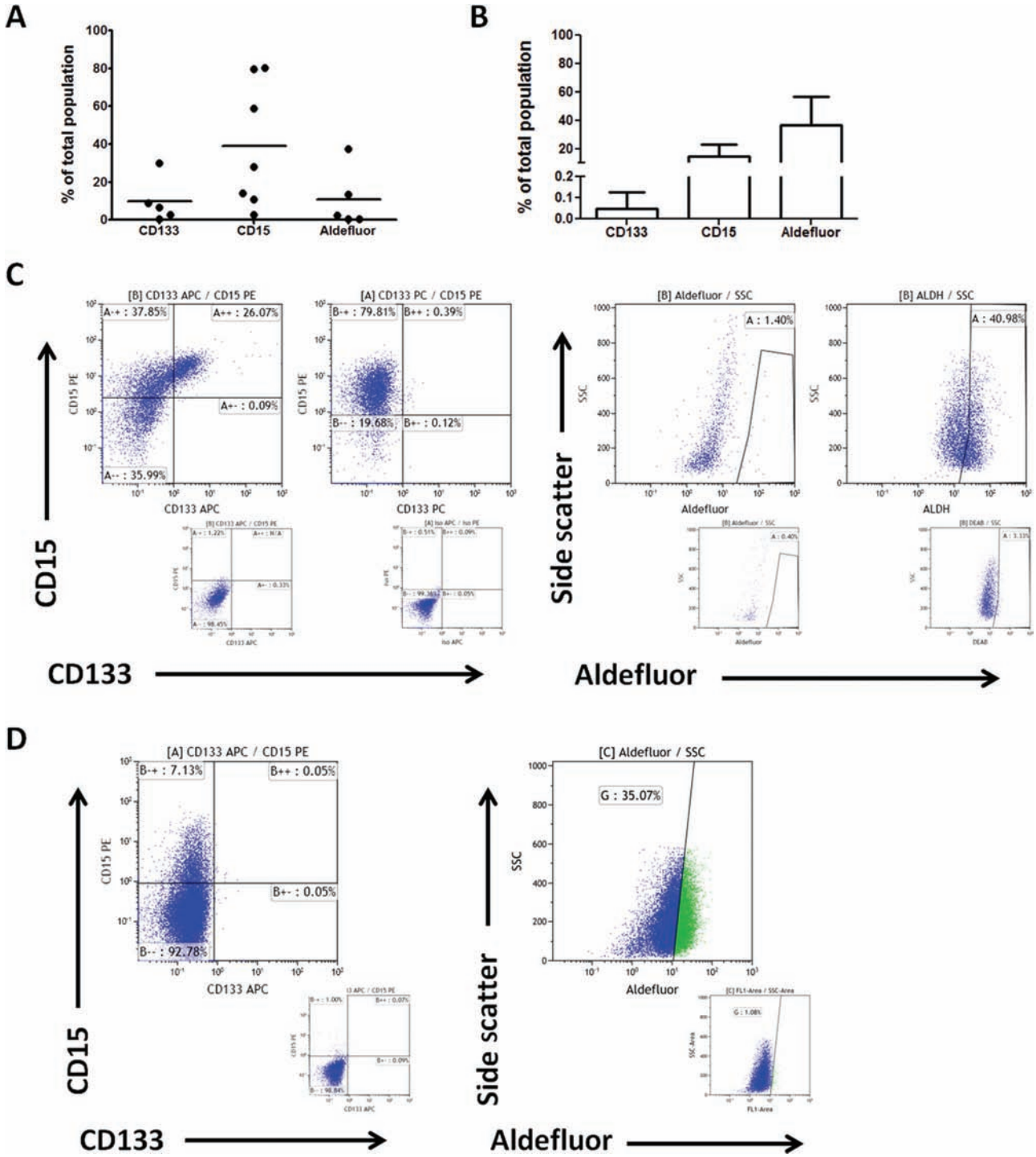

Figure 2. Brain tumor-initiating cell (BTIC) markers CD133 and aldehyde dehydrogenase (ALDH) are differentially expressed in patient-derived brain metastasis and NCI-H1915 tumorspheres. Tumorsphere cells were stained with CD133-APC, CD15-PE, and/or Aldefluor, and assessed by flow cytometry. Results are presented as mean ± SD. **A)** Patient-derived brain metastases (from lung) cultured in complete neural stem cell (cNSC) media. Each dot represents the percentage positive for a single patient sample; bar represents the mean of biological replicates: CD133, n = 5 (BT219, BT222, BT291, BT296, BT381); CD15, n = 7 (BT219, BT222, BT291, BT296, BT381, BT382, BT390); Aldefluor, n = 5 (BT296, BT298, BT382, BT390, BT397). **B)** The NCI-H1915 brain metastasis (from lung) cell line was cultured in cNSC media. The results of three independent experiments are shown as mean ± SD. **C-D)** Representative flow plots of patient samples (**left to right**) BT219 and BT381 (CD15 and CD133), and BT296 and BT390 (Aldefluor), **(C)** and the NCI-H1915 cell line **(D)** are shown. Plots from left to right are CD15-PE/CD133-APC, and side-scatter/Aldefluor, respective isotype, and DEAB (diethylaminobenzaldehyde) controls are shown below the corresponding flow plot.

Patient-Derived and NCI-H1915 Tumorspheres Form Multifocal Tumors in Mice After Intracranial Injection, Recapitulating Patient Brain Metastases

The gold standard for identification of a TIC population is serial tumor formation in immunocompromised mice (34). As such, we assessed tumor formation of patient-derived and NCI-H1915 tumorspheres with intracranial injections into NOD-SCID mice (n = 16 and n = 4, respectively). The cell line and patient samples behaved similarly in vivo, forming multifocal masses seeded throughout the ventricles and cerebellum (Figure 3A), despite being injected into the right frontal lobe. This is consistent with presentation of brain metastases in patients with metastatic lung cancer, in whom brain metastases are often multifocal, border the ventricles, and often develop in the cerebellum. The majority of injected patient samples formed tumors (Table 1), where xenografts recapitulated the patient tumor histology and cytoarchitecture (Figure 3B).

To further assess the degree to which the xenograft model recapitulates the original patient tumor, a subset of xenografts (n = 3) were stained with the same marker profile used to clinically diagnose patient brain metastases. Astonishingly, the staining profiles and patterns in the xenografts were identical to that of the original patient brain metastasis (Figure 3C, Table 1). This indicates that not only does injection of brain metastasis tumorspheres lead to the recapitulation of the patient tumor, but it also demonstrates that tumorsphere cells possess the TIC capacity to differentiate into the various tumor cell types in vivo.

NCI-H1915 Tumorsphere-Derived Tumors Are Serially Transplantable in NOD-SCID Mice

We next performed serial intracranial injections using NCI-H1915 tumorspheres to assess their ability to be serially passaged in vivo. Two parental (P1) tumors were processed and cultured to select for human stemlike tumor cells, as confirmed by flow cytometry analysis of EpCAM expression (data not shown). Three mice each were injected with 100 000 P1 tumor cells (n = 6 total). One of each P1 derivative from the subsequent (F1) tumors was similarly cultured and injected to give rise to F2 tumors (n = 6 total). F1 and F2 tumors resembled the histology and cytoarchitecture of the P1 tumors (Figure 4, A and B). Percentage of survival statistically significantly decreased with passaging (P = .02; Figure 4C), reflecting increased tumor growth rates. This may be a result of TIC outgrowth, or an artefact of in vivo selection for cells more adaptable to survival in a mouse neural microenvironment.

To address the issue of in vivo selection, we assessed sphere formation and expression of CD15 and CD133 on P1, F1, and F2 tumors. Outgrowth of a TIC population should be accompanied by increased sphere formation, and possibly increase expression of CD15 and/or CD133. Contrary to our prediction, experimental efforts to determine an increased TIC population were inconclusive (data not shown). This indicates that CD15 or CD133-expressing cells are not selected for during serial in vivo passaging, suggesting these may not be TIC markers of brain metastases. This is further supported by the absence of a difference in tumor formation, survival, and tumor phenotype of mice injected with $CD15^+$ or $CD15^-$ flow-sorted NCI-H1915 tumorsphere cells (Supplementary Figure 2, F–H, available online). Tumor formation suggests that there is likely a TIC population within brain metastases; however, in the case of NCI-H1915 tumorspheres, this population is not identifiable by BTIC marker expression.

Identification of Candidate Genes Overexpressed in Brain Metastasis Tumorspheres

After unsuccessful attempts to identify the TIC population in brain metastases using primary TIC markers, we wished to identify novel genes and/or pathways specifically overexpressed in brain metastasis tumorspheres. Two patient samples of brain metastasis (lung-derived) and early-passage BT241 tumorspheres were subjected to RNA-Seq (which is less noisy and requires fewer replicates than microarrays [46]) and subsequent analysis. Additional RNA-Seq data from two oligodendrogliomas (grade III primary brain tumors) and two primary lung tumors in the GSC Human Variation Database (47) were also used for comparative analysis. Comparisons between brain metastasis tumorspheres, primary lung and brain tumors were done to determine genes overexpressed exclusively in the brain metastasis stem cell population (Benjamini-Hochberg–adjusted q <.05). Thirty candidate genes were identified (Figure 5A), including genes involved in cell adhesion, cytoskeleton rearrangements, proliferation/tumorigenesis, and formation/disruption of cell–cell junctions.

To confirm their relevance to brain metastasis, we tested the predictive power of the candidate genes for overall patient survival, as poor survival of lung cancer patients strongly correlates with brain metastasis (2–5, 48). Because of our limited sample size, we examined patient survival in a larger homogenous dataset of 226 primary lung tumors (GSE31210). Of the 30 candidate genes, 25 were represented by the probeset used to acquire gene expression data in the dataset, and, as a whole, were associated with length of patient survival (P = .002, log-rank; Figure 5B). Due to its clinical implications, *EIF4EBP1* (Figure 5C), a repressor of mammalian target of rapamycin (mTOR)–mediated proliferation, where its repressive effects are relieved by phosphorylation by mTOR complex 1, was of particular interest (49). High levels of phosphorylated EIF4EBP1 are associated with poor clinical prognosis and increase proliferation in breast (50, 51) and ovarian (52) cancers.

We performed survival analysis with 25 candidate genes to identify which specific genes were related to patient survival, and found that elevated expression of 11 of 25 genes was statistically significantly associated with poor patient outcome (log-rank, $P \leq .05$; Figure 5D; Table 2). We also constructed a forward selection proportional hazard model, and identified four genes (*DSP*, *DSG2*, *NOC4L*, and *KRT7*) that optimally predicted patient outcome (log-rank, P = .001; Figure 5E). Although these genes may be useful for prognostic or diagnostic purposes, their functional involvement in disease has yet to be identified, warranting further study.

Discussion

Primary solid tumors have been shown to follow a CSC model of tumorigenesis, where TIC populations are exclusively responsible for tumor generation (9–22). In vitro, these CSC populations

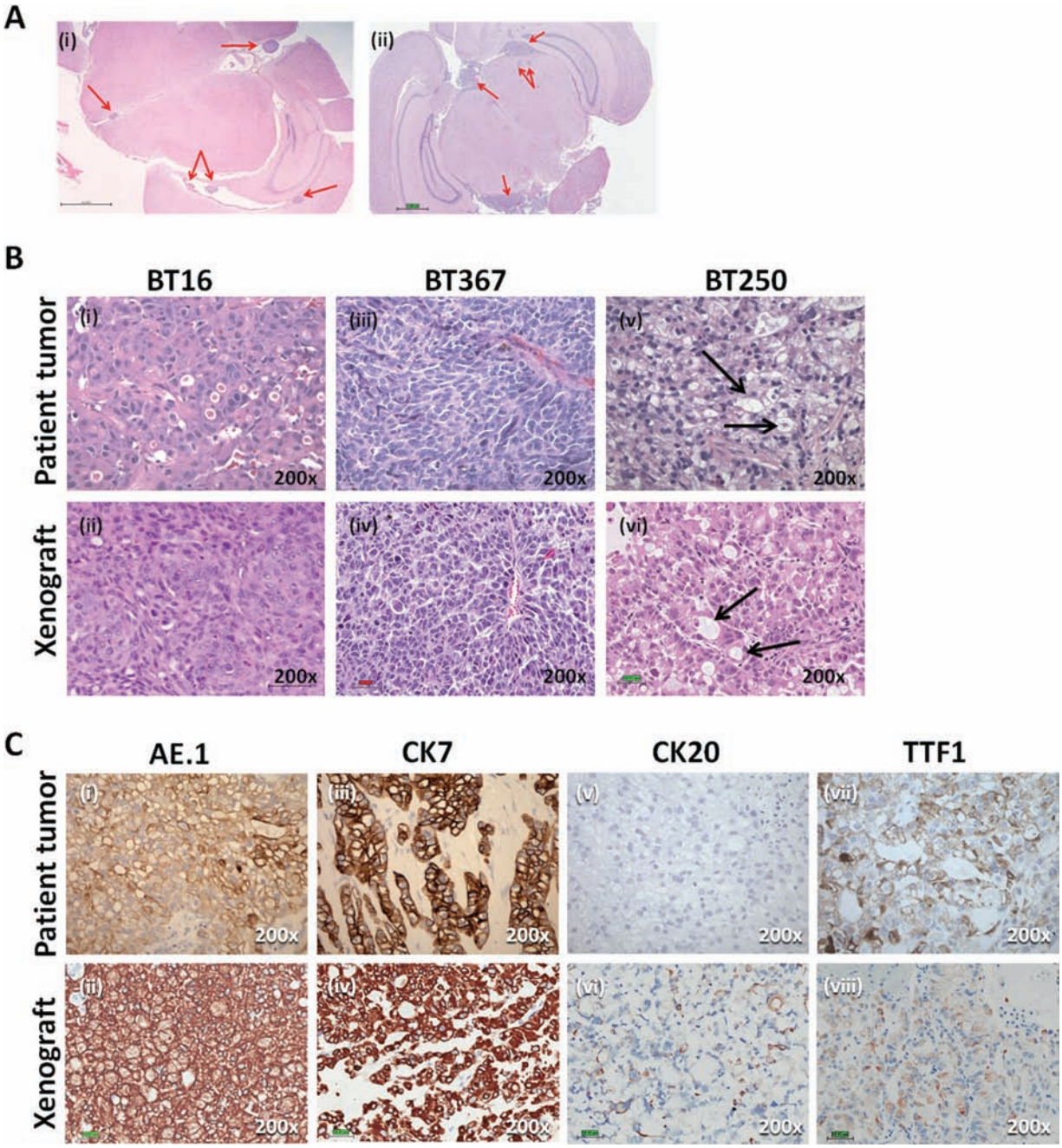

Figure 3. Tumorsphere cells from brain metastases are capable of recapitulating the original patient tumors when injected orthotopically into the frontal lobes of non-obese diabetic severe combined immunodeficient (NOD-SCID) mice. **A)** Intracranial injection of **(i)** patient-derived brain metastasis tumorsphere cells (BT16, 100 000 cells) and **(ii)** NCI-H1915 tumorsphere cells into NOD-SCID mice allows for the growth of multifocal masses seeded throughout the ventricles (**red arrows**), recapitulating the clinical presentation of patients with brain metastases. Representative hematoxylin-and-eosin (H&E)–stained sections are shown. **B)** High magnification comparison of matched patient tumors **(i, iii, and v)** and patient-derived xenografts **(ii, iv, and vii)** demonstrate maintenance of patient tumor histology and cytoarchitecture, including maintenance of clear-cell formations (**black arrows; v and vi**): **(i and ii)** BT16, 100 000 cells; **(iii and iv)** BT367, 180 000 cells; **(v-vi)** BT250, 100 000 cells. Representative H&E sections are shown; scale bar = 50 μm; magnification, ×200. **C)** Mouse xenografts of injected patient-derived brain metastasis tumorspheres were stained with the diagnostic profile used in the pathological diagnosis of patient brain metastases (**brown**, positive staining; **blue**, counterstain). Interestingly, xenografts stained with marker profiles and patterns identical to the original patient tumors. A representative matched patient–xenograft pair is shown (BT250, 100 000 cells). CK = cytokeratin; TTF1 = thyroid transcription factor 1; scale bar = 50 μm; magnification, ×200.

demonstrate increased self-renewal and differentiation into all tumor cell types; in vivo, TIC populations have the ability to serially recapitulate the original tumor. In this report, we demonstrate that brain metastases also possess such stemlike populations, as they have comparable sphere-forming capacity and stem cell frequency to primary brain tumor controls (Figure 1), are able initiate tumor growth, reproduce original tumor heterogeneity through in vivo differentiation, and can be serially passaged in vivo (Figures 3 and 4).

NCI-H1915 cells grown in stem-enriching cNSC conditions appear to be an appropriate model for the study of stem cell populations in brain metastases. Particularly valid assays include sphere

Table 1. Tumor formation of tumorsphere cells from patient-derived brain metastases*

Sample	Cell No.	Tumor formation	Xenograft profile	Patient profile
BT16	100 000	1 / 2	$CK7^{-}CK20^{-}AE.1^{-}TTF1^{-}$	$CK7^{-}$ $CK20^{-}$ $AE.1^{-}TTF1^{-}$
	50 000	2 / 2	n.d.	n.a.
BT69	34 000	2 / 4	n.d.	n.a.
BT250S	100 000	1 / 1	$CK7^{+}$ $CK20\text{-}AE.1^{+}TTF1^{+}$	$CK7^{+}$ $CK20^{-}$ $AE.1^{+}$ $TTF1^{+}$
	50 000	0 / 1	n.d.	n.a.
BT296	100 000	1 / 2†	n.d.	n.a.
BT367	180 000	1 / 1	$CK7^{-}$ $CK20^{-}$ $AE.1^{-}TTF1^{-}$	$CK7^{-}CK20^{-}$ $AE.1^{-}TTF1^{-}$
BT370	21 000	1 / 1†	n.d.	n.a.
BT381	200 000	1 / 1‡	n.d.	n.a.
BT382	275 000	1 / 1‡	n.d.	n.a.

* NOD-SCID mice were subjected to intracranial injection of the indicated numbers of tumor cells from patient samples. Tumor formation was based on hematoxylin-and-eosin staining of mouse brains upon reaching endpoint, the first of death or 6 months postinjection. n.d. = not determined; n.a. = not applicable; CK = cytokeratin; A.E.1 = cytokeratin cocktail (CKs 1–8, 10, 14–16, 19); TTF1 = thyroid transcription factor 1.

† Tumor cell infiltration into the cerebellum in the absence of a tumor mass.

‡ Cells injected into 4-week-old NOD-SCID gamma mice.

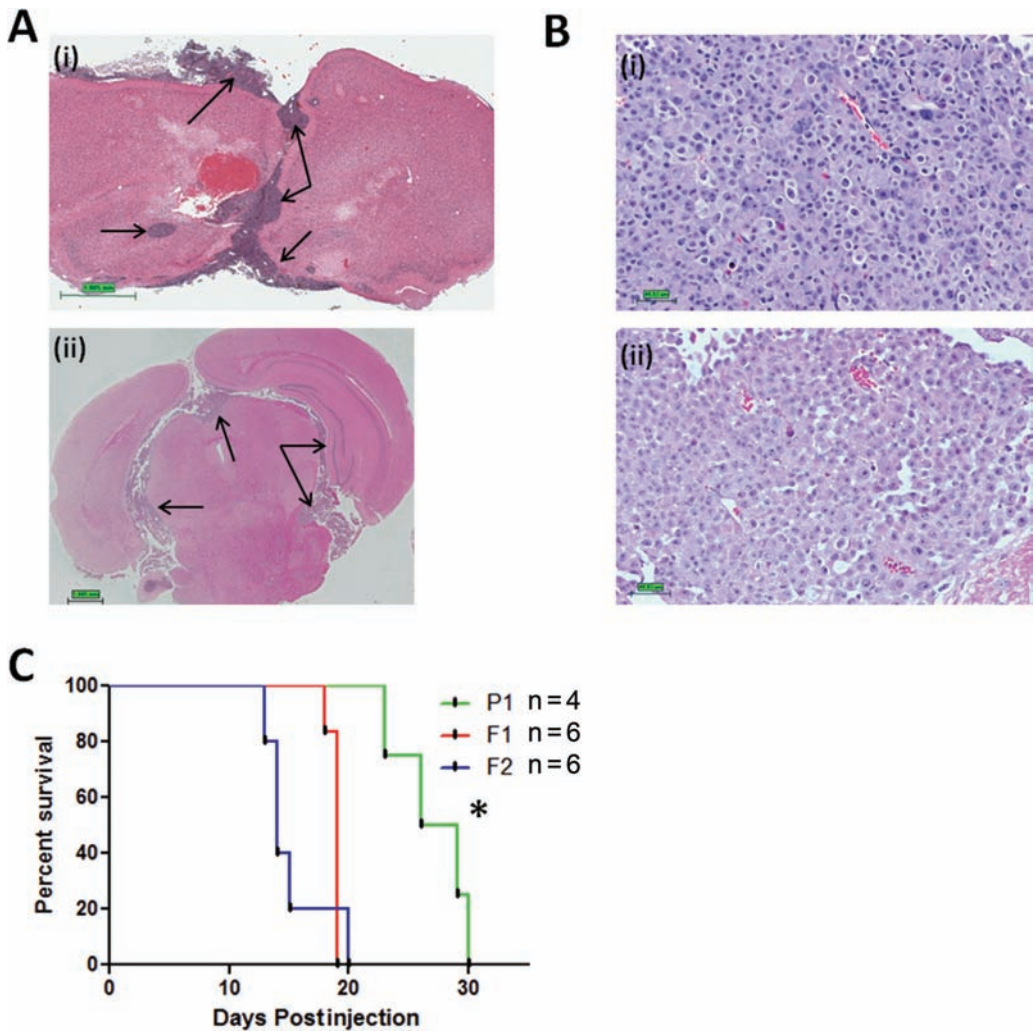

Figure 4. Serially transplanted tumorsphere-derived NCI-H1915 tumors resemble the parental tumor and lead to decreased survival. **A)** Serial injection of NCI-H1915 tumorsphere-derived parental tumors demonstrated growth patterns similar to the original tumor, F1 **(i)** and F2 **(ii)**. Representative hematoxylin-and-eosin (H&E) sections are shown; scale = 1 mm. **B)** NCI-H1915 tumors maintain the histology and cytoarchitecture seen in the P1 tumor **(i)** through in vivo passaging, F2 tumor **(ii)**. Representative H&E sections are shown; scale = 50 μm. **C)** Serially injected NCI-H1915 tumorsphere cells resulted in a statistically significant ($P = .02$) decrease in overall survival with subsequent injections (F1, F2; n = 6), compared to the initial injection (P1, n = 4). *$P < .05$.

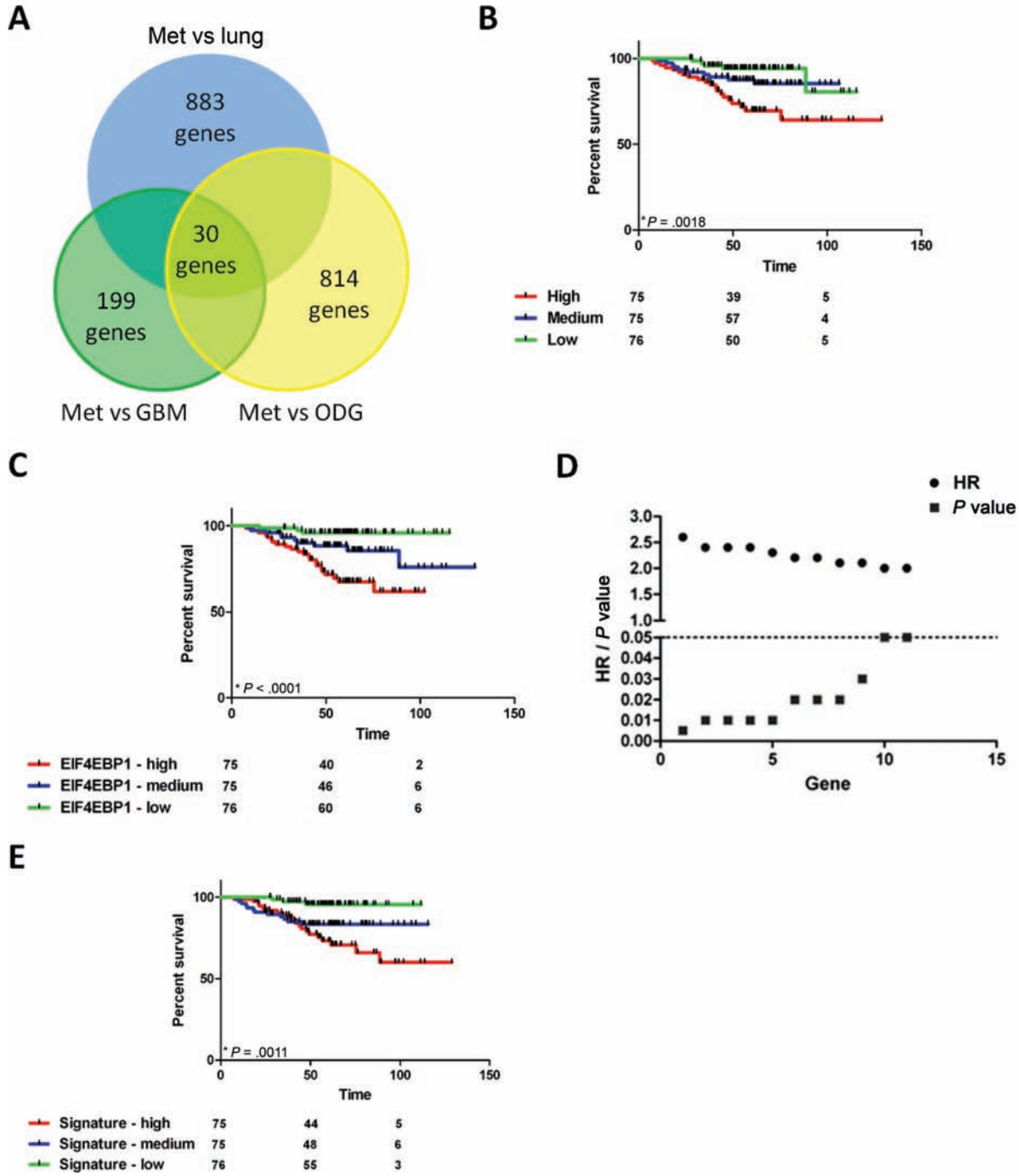

Figure 5. Identification of candidate genes overexpressed in brain metastasis tumorspheres from metastatic lung cancer, as compared to primary brain and lung tumors. RNA from two patient-derived brain metastasis tumorsphere cultures (BT219 and BT291 [Met]) and an early-passage tumorsphere culture of BT241 (GBM cell line [GBM]) were sent to Canada's Michael Smith Genome Sciences Centre (GSC) for transcriptome analysis using the Illumina platform. Normalized transcriptome profiles of the Met samples were compared to those of the GBM sample, primary lung (n = 2), and oligodendroglioma (ODG; n = 2) samples in the GSC database. **A)** Individual analyses between Met samples and GBM, ODG, and lung samples were done to identify genes that were statistically significantly overexpressed in brain metastases in each pairwise comparison (Benjamini-Hochberg–adjusted q <.05). **B)** Twenty-five of the 30 candidate genes were assessed in a dataset of 226 primary lung tumors (GSE31210) for their capacity to predict patient survival. **C)** The survival curve for *EIF4EBP1* is shown. **D)** Log-rank tests (median cut-point) of individual genes identified 11 genes that were statistically significantly associated with length of patient survival; $P \leq .05$ was considered to be statistically significant. **E)** Cox regression was used to perform stepwise regression, and identified four genes (DSP, DSG2, NOC4L, KRT7) as being an optimal model for predicting patient outcome. Time is expressed in months. HR = hazard ratio; red line = high signature expression (n = 75); blue line, medium signature expression (n = 75); green line = low signature expression (n = 76).

and tumor formation. Our system provides a much needed method to study brain metastases from the lung, and is unique in its application of the CSC model to in vitro and in vivo assay development. The minimally cultured tumorsphere-derived xenografts accurately recapitulate the patient tumor and may also provide a novel method with which to study the nascent metastatic cells. This cell

Table 2. Ranking of individual genes associated with lung cancer patient survival*

Gene	HR	*P*	Gene	HR	*P*
NOC4L	2.6	.005	CTSZ	---	n.s.
LAMC2	2.4	.01	RASAL1	---	n.s.
DSP	2.4	.01	IRF6	---	n.s.
MRPL3	2.4	.01	TCP1	---	n.s.
EIF4EBP1	2.3	.01	LPGAT1	---	n.s.
PLEKHG6	2.2	.02	NARS	---	n.s.
ZNF768	2.2	.02	RPS7	---	n.s.
MYH14	2.1	.02	CYC1	---	n.s.
KRT7	2.1	.03	SRC	---	n.s.
DSG2	2	.05	CTNND1	---	n.s.
MCRS1	2	.05	BAT3	---	n.s.
CAPN1	---	n.s.	PROM1	---	n.s.
SLC9A3R2	---	n.s.			

* Our 25 candidate genes were independently subjected to log-rank testing to determine their association with length of patient survival. Genes with *P* values ≤.05 were considered to be statistically significantly associated with length of patient survival; the HR for each of these genes is presented. HR = hazard ratio; n.s. = not statistically significant.

line may also be a suitable supply of cells when assessing the effects of new therapeutics on self-renewal or tumor growth.

Primary BTIC populations have been identified using cell surface markers CD133 and CD15, as well as the Aldefluor assay for ALDH activity. Our patient-derived brain metastasis and NCI-H1915 tumorspheres expressed these BTIC markers within or close to established ranges ($CD15^+$, 2.4%–70.5% [10, 13]; $CD133^+$, 19%–29% [12]; and $Aldefluor^+$, 4.8%–12.3% [14]); however, unlike in their primary brain tumor counterparts, none were useful in population segregation.

Recent studies have demonstrated equilibrium between stem and nonstem populations, where isolated nonstem populations can spontaneously convert to stemlike cells, reestablishing equilibrium (53–55). This dynamic relationship, along with other disadvantages of surface markers, such as glycosylation-dependent detection (56, 57), discrepancies in long- vs short-term culture (11, 12, 58), and lack of functionality, are likely reasons why they have yet to be explicitly applied to the study of metastasis.

Several reports suggest that stemlike cells of primary breast tumors may be intrinsically invasive in vitro, and metastatic in vivo (29, 30, 59–61), while others suggest that migratory cells can acquire self-renewal and tumorigenic capabilities through an epithelial–mesenchymal transition (62–66). Again, such seemingly dynamic relationships between cell populations indicate that targeting marker-specific populations in metastasis may not be ideal. In the case of brain metastasis, perhaps the best approach is to explore genes and signaling pathways required for the metastasis of lung cancer to the brain. In fact, using a breast-derived brain metastasis model, McGowan et al. demonstrate that depletion of $CD44^{hi}/CD24^{lo}$ CSCs, by inhibiting Notch signaling, led to less invasive behavior and fewer brain metastases (31). This suggests that not only are CSC populations relevant in brain metastases from other primary tumors, but also that these putative brain metastasis-initiating populations can be affected by disruption of important pathways.

Although some studies have identified organ-specific metastasis gene signatures from breast tumors, they neglect to study the candidate genes in the context of the CSC model, and depend on the potentially biased process of in vivo selection (67–71). Similar disadvantages surround gene signatures for lung metastasis to the brain (72). For the first time, we have identified prognostic candidate genes, based on their expression in stem cell-enriched brain metastasis patient samples. Similar patient-derived tumorspheres in the same stem-enriching conditions demonstrate stem cell properties of self-renewal and tumor formation, implicating the expression of these candidate genes in a CSC or TIC population. Survival analyses highlighted the importance of the 11 genes in the outcome of lung cancer patients, further implicating the importance and novelty of our brain metastasis tumorsphere-based signature.

It is important to note that only the NCI-H1915 cell line was used to establish our in vitro and in vivo CSC models of brain metastases. The only alternate commercial cell line was neither biologically relevant (small cell carcinoma), nor viable in cNSC conditions. We emphasize that a single cell line is not necessarily representative of the intertumor variation seen in patients; therefore, findings of any work performed using NCI-H1915 cells should be confirmed through validation in a subset of patient samples or patient-derived cell lines. Other limitations of this study include the fact that identification of our candidate genes was limited by our small sample size. Despite validation using survival analyses in much larger datasets, we were unable to determine their direct prognostic value for the occurrence of brain metastases. Additional functional studies are required to make definitive conclusions for the prediction of brain metastasis.

Through characterization of genes and pathways essential for the metastasis of lung cancer to the brain, not only in the context of invasion and metastasis, but also in that of the CSC model, more effective targets may be identified. Not only would such genes and pathways be useful therapeutic targets, but it is also possible that they may be expressed in the rare subset of cells that successfully form brain metastases from the bulk primary tumor. Identification of a putative brain metastasis-initiating population would not only provide an alternative therapeutic target to genes or pathways, but would also help elucidate the relationship between TIC and metastatic potential, as it has been suggested that these are divergent characteristics (73). By blocking the metastatic process, formation of brain and other metastases could be prevented, transforming a systemic and fatal disease into a locally controlled and much more treatable one.

References

1. Schouten LJ, Rutten J, Huveneers HA, Twijnstra A. Incidence of brain metastases in a cohort of patients with carcinoma of the breast, colon, kidney, and lung and melanoma. *Cancer*. 2002;94(10):2698–2705.
2. Sorensen JB, Hansen HH, Hansen M, Dombernowsky P. Brain metastases in adenocarcinoma of the lung: frequency, risk groups, and prognosis. *J Clin Oncol*. 1988;6(9):1474–1480.
3. Quint LE, Tummala S, Brisson LJ, et al. Distribution of distant metastases from newly diagnosed non-small cell lung cancer. *Ann Thorac Surg*. 1996;62(1):246–250.
4. Cox JD, Yesner RA. Adenocarcinoma of the lung: recent results from the Veterans Administration Lung Group. *Am Rev Respir Dis*. 1979;120(5):1025–1029.
5. Komaki R, Cox JD, Stark R. Frequency of brain metastasis in adenocarcinoma and large cell carcinoma of the lung: correlation with survival. *Int J Radiat Oncol Biol Phys*. 1983;9(10):1467–1470.

6. Wilkins RH, Rengachary, SS, ed. *Neurosurgery*. 2nd ed. Toronto: McGraw-Hill; 1996; No. 1.
7. Gavrilovic IT, Posner JB. Brain metastases: epidemiology and pathophysiology. *J Neurooncol*. 2005;75(1):5–14.
8. Maher EA, Mietz J, Arteaga CL, DePinho RA, Mohla S. Brain metastasis: opportunities in basic and translational research. *Cancer Res*. 2009;69(15):6015–6020.
9. Rasper M, Schafer A, Piontek G, et al. Aldehyde dehydrogenase 1 positive glioblastoma cells show brain tumor stem cell capacity. *Neuro Oncol*. 2010;12(10):1024–1033.
10. Mao XG, Zhang X, Xue XY, et al. Brain tumor stem-like cells identified by neural stem cell marker CD15. *Transl Oncol*. 2009;2(4):247–257.
11. Singh SK, Clarke ID, Terasaki M, et al. Identification of a cancer stem cell in human brain tumors. *Cancer Res*. 2003;63(18):5821–5828.
12. Singh SK, Hawkins C, Clarke ID, et al. Identification of human brain tumour initiating cells. *Nature*. 2004;432(7015):396–401.
13. Son MJ, Woolard K, Nam DH, Lee J, Fine HA. SSEA-1 is an enrichment marker for tumor-initiating cells in human glioblastoma. *Cell Stem Cell*. 2009;4(5):440–452.
14. Bar EE, Chaudhry A, Lin A, et al. Cyclopamine-mediated hedgehog pathway inhibition depletes stem-like cancer cells in glioblastoma. *Stem Cells*. 2007;25(10):2524–2533.
15. Eramo A, Lotti F, Sette G, et al. Identification and expansion of the tumorigenic lung cancer stem cell population. *Cell Death Differ*. 2008;15(3):504–514.
16. O'Brien CA, Pollett A, Gallinger S, Dick JE. A human colon cancer cell capable of initiating tumour growth in immunodeficient mice. *Nature*. 2007;445(7123):106–110.
17. Al-Hajj M, Wicha MS, Benito-Hernandez A, Morrison SJ, Clarke MF. Prospective identification of tumorigenic breast cancer cells. *Proc Natl Acad Sci U S A*. 2003;100(7):3983–3988.
18. Ricci-Vitiani L, Lombardi DG, Pilozzi E, et al. Identification and expansion of human colon-cancer-initiating cells. *Nature*. 2007;445(7123):111–115.
19. Ginestier C, Hur MH, Charafe-Jauffret E, et al. ALDH1 is a marker of normal and malignant human mammary stem cells and a predictor of poor clinical outcome. *Cell Stem Cell*. 2007;1(5):555–567.
20. Huang EH, Hynes MJ, Zhang T, et al. Aldehyde dehydrogenase 1 is a marker for normal and malignant human colonic stem cells (SC) and tracks SC overpopulation during colon tumorigenesis. *Cancer Res*. 2009;69(8):3382–3389.
21. Chen YC, Chen YW, Hsu HS, et al. Aldehyde dehydrogenase 1 is a putative marker for cancer stem cells in head and neck squamous cancer. *Biochem Biophys Res Commun*. 2009;385(3):307–313.
22. Liang D, Shi Y. Aldehyde dehydrogenase-1 is a specific marker for stem cells in human lung adenocarcinoma. *Med Oncol*. 2012;29(2):633–639.
23. Kim CF, Jackson EL, Woolfenden AE, et al. Identification of bronchioalveolar stem cells in normal lung and lung cancer. *Cell*. 2005;121(6):823–835.
24. Sutherland KD, Berns A. Cell of origin of lung cancer. *Mol Oncol*. 2010;4(5):397–403.
25. Hong KU, Reynolds SD, Watkins S, Fuchs E, Stripp BR. Basal cells are a multipotent progenitor capable of renewing the bronchial epithelium. *Am J Pathol*. 2004;164(2):577–588.
26. Croker AK, Allan AL. Cancer stem cells: implications for the progression and treatment of metastatic disease. *J Cell Mol Med*. 2008;12(2):374–390.
27. Kienast Y, von Baumgarten L, Fuhrmann M, et al. Real-time imaging reveals the single steps of brain metastasis formation. *Nat Med*. 2010;16(1):116–122.
28. Luzzi KJ, MacDonald IC, Schmidt EE, et al. Multistep nature of metastatic inefficiency: dormancy of solitary cells after successful extravasation and limited survival of early micrometastases. *Am J Pathol*. 1998;153(3):865–873.
29. Croker AK, Goodale D, Chu J, et al. High aldehyde dehydrogenase and expression of cancer stem cell markers selects for breast cancer cells with enhanced malignant and metastatic ability. *J Cell Mol Med*. 2009;13(8B):2236–2252.
30. Liu H, Patel MR, Prescher JA, et al. Cancer stem cells from human breast tumors are involved in spontaneous metastases in orthotopic mouse models. *Proc Natl Acad Sci U S A*. 2010;107(42):18115–18120.
31. McGowan PM, Simedrea C, Ribot EJ, et al. Notch1 inhibition alters the CD44hi/CD24lo population and reduces the formation of brain metastases from breast cancer. *Mol Cancer Res*. 2011;9(7):834–844.
32. Davis SJ, Divi V, Owen JH, et al. Metastatic potential of cancer stem cells in head and neck squamous cell carcinoma. *Arch Otolaryngol Head Neck Surg*. 2010;136(12):1260–1266.
33. Chen C, Wei Y, Hummel M, et al. Evidence for epithelial-mesenchymal transition in cancer stem cells of head and neck squamous cell carcinoma. *PLoS One*. 2011;6(1):e16466.
34. Clarke MF, Dick JE, Dirks PB, et al. Cancer stem cells—perspectives on current status and future directions: AACR Workshop on cancer stem cells. *Cancer Res*. 2006;66(19):9339–9344.
35. Tropepe V, Sibilia M, Ciruna BG, Rossant J, Wagner EF, van der Kooy D. Distinct neural stem cells proliferate in response to EGF and FGF in the developing mouse telencephalon. *Dev Biol*. 1999;208(1):166–188.
36. Reynolds BA, Weiss S. Clonal and population analyses demonstrate that an EGF-responsive mammalian embryonic CNS precursor is a stem cell. *Dev Biol*. 1996;175(1):1–13.
37. Okayama H, Kohno T, Ishii Y, et al. Identification of genes upregulated in ALK-positive and EGFR/KRAS/ALK-negative lung adenocarcinomas. *Cancer Res*. 2012;72(1):100–111.
38. Irizarry RA, Hobbs B, Collin F, et al. Exploration, normalization, and summaries of high density oligonucleotide array probe level data. *Biostatistics*. 2003;4(2):249–264.
39. Hallett RM, Dvorkin-Gheva A, Bane A, Hassell JA. A gene signature for predicting outcome in patients with basal-like breast cancer. *Sci Rep*. 2012;2:227.
40. Yau C, Esserman L, Moore DH, Waldman F, Sninsky J, Benz CC. A multigene predictor of metastatic outcome in early stage hormone receptor-negative and triple-negative breast cancer. *Breast Cancer Res*. 2010;12(5):R85.
41. Inagaki A, Soeda A, Oka N, et al. Long-term maintenance of brain tumor stem cell properties under at non-adherent and adherent culture conditions. *Biochem Biophys Res Commun*. 2007;361(3):586–592.
42. Wu W, He Q, Li X, et al. Long-term cultured human neural stem cells undergo spontaneous transformation to tumor-initiating cells. *Int J Biol Sci*. 2011;7(6):892–901.
43. Deng S, Yang X, Lassus H, et al. Distinct expression levels and patterns of stem cell marker, aldehyde dehydrogenase isoform 1 (ALDH1), in human epithelial cancers. *PLoS One*. 2010;5(4):e10277.
44. Jiang F, Qiu Q, Khanna A, et al. Aldehyde dehydrogenase 1 is a tumor stem cell-associated marker in lung cancer. *Mol Cancer Res*. 2009;7(3):330–338.
45. Capela A, Temple S. LeX/ssea-1 is expressed by adult mouse CNS stem cells, identifying them as nonependymal. *Neuron*. 2002;35(5):865–875.
46. Mortazavi A, Williams BA, McCue K, Schaeffer L, Wold B. Mapping and quantifying mammalian transcriptomes by RNA-Seq. *Nat Methods*. 2008;5(7):621–628.
47. Fejes AP, Khodabakhshi AH, Birol I, Jones SJ. Human variation database: an open-source database template for genomic discovery. *Bioinformatics*. 2011;27(8):1155–1156.
48. Sen M, Demiral AS, Cetingoz R, et al. Prognostic factors in lung cancer with brain metastasis. *Radiother Oncol*. 1998;46(1):33–38.
49. Fingar DC, Blenis J. Target of rapamycin (TOR): an integrator of nutrient and growth factor signals and coordinator of cell growth and cell cycle progression. *Oncogene*. 2004;23(18):3151–3171.
50. Rojo F, Najera L, Lirola J, et al. 4E-binding protein 1, a cell signaling hallmark in breast cancer that correlates with pathologic grade and prognosis. *Clin Cancer Res*. 2007;13(1):81–89.
51. Pons B, Peg V, Vazquez-Sanchez MA, et al. The effect of p-4E-BP1 and p-eIF4E on cell proliferation in a breast cancer model. *Int J Oncol*. 2011;39(5):1337–1345.
52. Castellvi J, Garcia A, Rojo F, et al. Phosphorylated 4E binding protein 1: a hallmark of cell signaling that correlates with survival in ovarian cancer. *Cancer*. 2006;107(8):1801–1811.
53. Gupta PB, Fillmore CM, Jiang G, et al. Stochastic state transitions give rise to phenotypic equilibrium in populations of cancer cells. *Cell*. 2011;146(4):633–644.

54. Scaffidi P, Misteli T. In vitro generation of human cells with cancer stem cell properties. *Nat Cell Biol*. 2011;13(9):1051–1061.
55. Chaffer CL, Brueckmann I,Scheel C, et al. Normal and neoplastic nonstem cells can spontaneously convert to a stem-like state. *Proc Natl Acad Sci U S A*. 2011;108(19):7950–7955.
56. Kemper K, Sprick MR, de Bree M, et al. The AC133 epitope, but not the CD133 protein, is lost upon cancer stem cell differentiation. *Cancer Res*. 2010;70(2):719–729.
57. Osmond TL, Broadley KW, McConnell MJ. Glioblastoma cells negative for the anti-CD133 antibody AC133 express a truncated variant of the CD133 protein. *Int J Mol Med*. 2010;25(6):883–888.
58. Chen R, Nishimura MC, Bumbaca SM, et al. A hierarchy of self-renewing tumor-initiating cell types in glioblastoma. *Cancer Cell*. 17(4):362–375.
59. Charafe-Jauffret E, Ginestier C, Iovino F, et al. Aldehyde dehydrogenase 1-positive cancer stem cells mediate metastasis and poor clinical outcome in inflammatory breast cancer. *Clin Cancer Res*. 2010;16(1):45–55.
60. Marcato P, Dean CA, Pan D, et al. Aldehyde dehydrogenase activity of breast cancer stem cells is primarily due to isoform ALDH1A3 and its expression is predictive of metastasis. *Stem Cells*. 2011;29(1):32–45.
61. Sheridan C, Kishimoto H, Fuchs RK, et al. CD44+/CD24- breast cancer cells exhibit enhanced invasive properties: an early step necessary for metastasis. *Breast Cancer Res*. 2006;8(5):R59.
62. Fang X, Cai Y, Liu J, et al. Twist2 contributes to breast cancer progression by promoting an epithelial-mesenchymal transition and cancer stem-like cell self-renewal. *Oncogene*. 2011;30(47):4707–4720.
63. Hwang WL, Yang MH, Tsai ML, et al. SNAIL regulates interleukin-8 expression, stem cell-like activity, and tumorigenicity of human colorectal carcinoma cells. *Gastroenterology*. 2011;141(1):279–291.
64. Mani SA, Guo W, Liao MJ, et al. The epithelial-mesenchymal transition generates cells with properties of stem cells. *Cell*. 2008;133(4):704–715.
65. Vesuna F, Lisok A, Kimble B, Raman V.Twist modulates breast cancer stem cells by transcriptional regulation of CD24 expression. *Neoplasia*. 2009;11(12):1318–1328.
66. Yang MH, Hsu DS, Wang HW, et al. Bmi1 is essential in Twist1-induced epithelial-mesenchymal transition. *Nat Cell Biol*. 2010;12(10):982–992.
67. Minn AJ, Gupta GP, Siegel PM, et al. Genes that mediate breast cancer metastasis to lung. *Nature*. 2005;436(7050):518–524.
68. Minn AJ, Kang Y, Serganova I, et al. Distinct organ-specific metastatic potential of individual breast cancer cells and primary tumors. *J Clin Invest*. 2005;115(1):44–55.
69. Kang Y, Siegel PM, Shu W, et al. A multigenic program mediating breast cancer metastasis to bone. *Cancer Cell*. 2003;3(6):537–549.
70. Bos PD, Zhang XH, Nadal C, et al. Genes that mediate breast cancer metastasis to the brain. *Nature*. 2009;459(7249):1005–1009.
71. Minn AJ, Gupta GP, Padua D, et al. Lung metastasis genes couple breast tumor size and metastatic spread. *Proc Natl Acad Sci U S A*. 2007;104(16):6740–6745.
72. Nguyen DX, Chiang AC, Zhang XH, et al. WNT/TCF signaling through LEF1 and HOXB9 mediates lung adenocarcinoma metastasis. *Cell*. 2009;138(1):51–62.
73. Wu X, Northcott PA, Dubuc A, et al. Clonal selection drives genetic divergence of metastatic medulloblastoma. *Nature*. 2012;482(7386):529–533.

Funding

This work was supported by the McMaster University Department of Surgery (not applicable), the Canadian Cancer Society Research Institute (2012–701052), and the Ontario Institute for Cancer Research (CSC-PRAR-MAC).

Note

We thank Bernardo Trigatti and Katrin Scheinemann for their excellent discussion and experimental recommendations for this manuscript, and the Hamilton Regional Lab Medicine Program for performing the immunohistochemistry on our samples.

Affiliations of authors: Department of Biochemistry and Biomedical Sciences (SMN, CV, RMH, BM, JAH, SKS), Department of Neuroscience (EO, SKS), Department of Surgery (NKM, PK, EK, SKS), Department of Pathology and Molecular Medicine (JPP), Department of Health Research Methodology (FF),and Department of Pediatrics (SKS), Faculty of Health Sciences, McMaster Stem Cell and Cancer Research Institute (SMN, CV, NM, EO, BM, SKS), and McMaster Centre of Functional Genomics (RMH, JAH), McMaster University, Hamilton, ON, Canada; Genome Sciences Centre, BC Cancer Agency (OM, MM), and Department of Medical Genetics, University of British Columbia (MM), Vancouver, BC, Canada.